Topical Application of Houttuynia Cordata Thunb Ethanol Extracts Increases Tumor Infiltrating CD8+/Treg Cells Ratio and Inhibits Cutaneous Squamous Cell Carcinoma In Vivo

Lipeng Gao
Shanghai University

Rong-Yin Gui
Shanghai University

Xin-Nan Zheng
Shanghai University

Ying-Xue Wang
Shanghai University

Yao Gong
Shanghai University

Tim Hua Wang
Shanghai University

Jichuan Wang
Fujian Medical University

Junyi Huang
Shanghai University

Xin-Hua Liao (✉ xinhualiao@foxmail.com)
Shanghai University   https://orcid.org/0000-0001-7520-7135

Abstract

Houttuynia cordata Thunb (HCT) is a medicinal and edible herb which has beneficial effects on various diseases due to its diuretic, anti-inflammatory, anti-oxidative, anti-microbial, anti-viral, anti-cancer and anti-diabetic properties. Most of reports of its anti-cancer activity were conducted in vitro, and its effects on cutaneous squamous cell carcinoma (SCC) has not been investigated yet. Using DMBA/TPA induced SCC mice model, we found that topical treatment by HCT, as well as its bioactive ingredient monomer, efficiently inhibited tumor growth. Mechanistically, we found tumor infiltrating CD4^{+}, Foxp3^{+} T regulatory cells (Tregs) were significantly reduced and CD8^{+}/Treg cells ratio was largely increased in tumors after HCT treatment. In addition, several chemokines which recruited immune cells were largely reduced when SCC cancer cells were treated by HCT in vitro. Our results demonstrate the therapeutic effects of HCT on cutaneous SCC and indicate it might inhibit cancer through regulating tumor infiltrating lymphocytes and the tumor immune microenvironments.

Introduction

Houttuynia cordata Thunb (HCT) is a well-known traditional Chinese medicinal and edible herb, which possesses a variety of pharmacological activities including diuretic, anti-microbial, anti-viral, anti-diabetic, anti-inflammatory, anti-oxidative, anti-mutagenic and anti-cancer properties [1, 2]. It has shown therapeutic effect on many diseases including inflammation, pneumonia, severe acute respiratory syndrome (SARS), muscular sprain, cancer, obesity, stomach ulcer and cancer [1, 2]. HCT has inhibitory effects on cell growth of colon cancer [3], gastric cancer [4], melanoma [5], hepatocellular carcinoma [6], breast cancer [7], colorectal cancer [8], lung cancer [9] and leukemia in vitro [10]. HCT also exhibits inhibitory activity on lung cancer in vivo [11]. However, it has not been studied in non-melanoma skin cancer yet.

Skin cancer is the most common cancer worldwide [12, 13]. Basal cell carcinoma (BCC) and squamous cell carcinoma (SCC) are the most common forms in non-melanoma skin cancer. In comparison with BCC, SCC is more malignant and has potential to recur and metastasize to other tissues and organs [12, 13]. The incidence of SCC has been increased over the past decades [12, 14]. Most of SCC can be surgically removed. Radiotherapy and chemotherapy might be used as an adjunct to surgery in advanced SCC patients, if surgery is contraindicated, or if tumor is located in cosmetically sensitive area [15]. There is still a lack of safe and effective medicine for treating malignant SCC.

Exposure to ultra-violet radiation is the most common cause of SCC. Other risk factors include exposure to radiation, carcinogenic chemicals, chronic skin ulceration, and immunosuppressive medication [16]. SCC development is a multistep process which consists of DNA mutation, genome instability, epigenetic changes, inflammation, oxidative stress and tumor microenvironment changes [16–19]. Mice SCC can be induced by two-stage carcinogenesis protocols which employ mutagenic chemical 7, 12-diemthylbenz[a]anthracene (DMBA) as initiators and proinflammatory chemical 12-O-tetradecanoylphorbol-13-acetate (TPA) as promoters [20]. This mouse model mimics human SCC

exposed to UV or other carcinogens. Large-scale whole exon sequencing revealed that many DNA mutations induced by DMBA/TPA are consistent with mutations in human SCC [21]. In mice SCC model, tumors on back skin can be directly visualized, quantitatively measured and therefore traced individually over time. In addition, drug can be topically applied onto skin, therefore better reach the tumor cells to execute its anti-cancer activity. As we know, drugs are metabolized about 10 times faster in mice than human [22]. Systematic application of drugs often shows no or mild activity in mice, owing that the drugs could not reach the therapeutic concentration in blood. Traditional medicine usually uses the whole plant extracts instead of monomer to treat diseases. They often only show mild to moderate therapeutic effects in human, and these effects might not be observed in mice if they are systematically applied. Thus, chemical induced mice SCC is an ideal model to evaluate the anti-cancer activity of traditional medicine by topical application.

Cancer cells grow in a special microenvironment where tumor associated cells (immune cells, fibroblast etc.) and cancer cells interact with each other to reach a balance between suppression and tolerance of cancer cells growth. Infiltrating immune cells are major constituents of the tumor microenvironment which play important roles in tumor development, invasion, metastasis, and outcome. Among these infiltrating cells, $CD8^+$ effector T cells are capable of killing cancer cells, while $CD4^+$, $Foxp3^+$ T regulatory cells (Tregs or T_{reg} cells) secrete a variety of immunosuppressive cytokines, which dampen induction and proliferation of effector T cells [23]. Cancer cells alter the normal homeostatic ratio of effector to regulatory T cells and evade immune surveillance. High infiltrating $CD8^+$/Treg cells ratios is associated with better prognosis and better response to chemotherapy and immunotherapy in various cancer types [24]. HCT is able to reduce tissue infiltrating inflammatory cells. In rat carrageenan-air pouch model, oral administration of supercritical extracts of HCT suppressed carrageenan-induced exudation as well as inflammatory cell infiltration [25]. In influenza A virus induced acute lung injury mice model, the lungs treated by flavonoid glycosides extracted from HCT presented milder inflammatory infiltration [26]. However, it has not been examined whether HCT treatment can alter the tumor infiltrating lymphocytes and tumor immune microenvironment.

In this study, we used mice SCC model to examine anti-cancer activity of HCT and one of its bioactive ingredients sodium new houttuyfonate (SNH). We used chemical DMBA/TPA to induce SCC and then applied ethanol extracts of HCT or SNH onto back skin. In comparison with control group, the SCC growth was significantly reduced without affecting mice body weight, indicating low toxic effects of HCT and SNH. Mechanistically, we found tumor infiltrating $CD8^+$ and $CD4^+$ T cells were both reduced after HCT treatment. More significantly, $CD8^+$/Treg cells ratio was largely increased. Our data demonstrate that HCT is a potential drug for treating cutaneous SCC, and indicate it might inhibit tumor growth through regulating tumor immune microenvironment.

Materials And Methods

Animals

ICR mice were obtained from Shanghai SLAC Laboratory Animal Co., Ltd and housed under SPF conditions. All experiments involving animals were performed in accordance with the guidelines of the Institutional Animal Care and Use Committee (IACUC) of Shanghai University (the protocol number: 2019033).

Materials

7, 12-diemthylbenz[a]anthracene (DMBA) and 12-O-tetradecanoylphorbol-13-acetate (TPA) were purchased from Sigma-Aldrich, Inc. Dried HCT whole plants were purchased from Jiangxi Qirentang Chinese Herbal Slices Co., Ltd. Sodium new houttuyfonate (SNH, purity≥98%) was purchased from Shanghai Yuanye Bio-technology Co. Ltd. Vendor and catalog information of antibodies against the following proteins are listed here: β−Catenin (#8480S, Cell Signaling Tech), Actin (#HC201, TransGen Biotech), ERK2 (#A0229, Abclonal Tech), ABCG2 (#A5661, Abclonal Tech), CD4 (for Western blot, #bs-0766R, Beijing Biosynthesis Biotech), CD8 (for Western blot, #bs-10699R, Beijing Biosynthesis Biotech); CD4 (conjugated with Alexa Fluor 700, for immunostaining, #53-0041-80, Thermo Fisher Scientific), CD8 (conjugated with Alexa Fluor 488, for immunostaining, #553-0081-80, Thermo Fisher Scientific), FoxP3 (conjugated with Alexa Fluor 488, for immunostaining, #126405, Biolegend).

Preparation of Houttuynia cordata Thunb ethanol extracts

The dried whole plants were grounded into powders, which were then immersed in 95% ethanol (3 ml of 95% ethanol per 1g of powder) with stirring at room temperature overnight. The mixture was then centrifuged at 2800 x g and filtered through Whatman filter paper. Finally, the ethanol extracts were lyophilized by rotary evaporator. The final solid extracts were stored at − 20 °C. Before use, solid extracts were re-dissolved in organic solvent DMSO.

Mice skin carcinogenesis model and treatment

Two-stage model of skin tumorigenesis was employed to induce skin cancer. Back skin of 6-Week-old female ICR mice were shaved and then applied topically with DMBA (100 nmol/300 mL of acetone) twice weekly for two weeks, followed by TPA (10 nmol/300 μL of DMSO) twice weekly for six weeks. When tumor appeared, tumor length (L) and width (W) were measured twice a week by vernier caliper. The tumor volume (TV) was calculated according to the formula TV = $(L \times W^2)/2$. The total tumor volume of each mouse is the sum of all of tumors on back skin. When average total tumor volume of each mouse reached ~100 mm^3, 14 mice with similar total tumor volume were selected and divided into HCT treatment and control groups. The two groups had similar average total tumor volume and distribution. Thereafter, the mice were treated with HCT ethanol extracts or the control solvent daily by topical application for another three weeks. TPA would not be further applied during HCT treatment.

In addition, SNH was dissolved in 75 °C ddH$_2$O as a 100 mg/kg stock solution and stored at 4 °C. When average total tumor volume of each mouse reached ~100 mm^3, 27 mice with similar total tumor volume were selected and divided into SNH (20 mg/kg), SNH (100 mg/kg) and control groups. The three groups

had similar average total tumor volume and distribution. Thereafter, the mice were treated with SNH or the control water daily by topical application for another five weeks. TPA would not be further applied during SNH treatment.

TPA-induced skin thickening in mice

Back skin of 6-Week-old female ICR mice (n = 6) were shaved and preteated with topical application of HCT ethanol extracts or the control solvent daily for 10 days, followed by TPA (10 nmol/300 μL of DMSO) topical application daily for 3 days. Skin was then harvested for further analysis.

Western blot analysis of tumor samples

After three weeks of treatment, mice from HCT and control groups were euthanized and the tumors with similar volume were harvested by scissors. Tumor samples were grounded in liquid nitrogen and dissolved in RIPA lysates containing protease inhibitors. Samples were then sonicated and centrifugated. The supernatant was aspirated and mixed with SDS-loading buffer for further analysis. Protein samples (20-35 μg) were resolved on 12% Tris-glycine gels and transferred onto a nitrocellular membrane. After blocking, the membrane was incubated with the primary antibody and then horseradish peroxidase (HRP)-conjugated secondary antibody. After washing, the HRP substrate was added and the chemiluminescence signal was detected by a CCD camera.

Hematoxylin and eosin (H&E) staining

Briefly, tumor samples were embedded in paraffin, sectioned and dewaxed. After samples were hydrated, they were stained with hematoxylin and eosin. The samples were dehydrated and then applied with Permount/Toluene solution, covered with coverslip and sealed by nail polish. Images were captured using optical microscope.

Immunostaining

Tumor samples were embedded and frozen on dry ice in OCT compound (Sakura Finetek) and then sectioned at 6-9 μm. Sample sections were then fixed in 4% PFA and stained with Alexa Fluor conjugated antibodies. Fluorescence images were visualized and captured by fluorescent microscopy.

Real-time Quantitative PCR

The total RNA of the human A431 cells was isolated with TRIzol (Ambion, USA) and reverse-transcribed to cDNA by an iScript Select cDNA Synthesis Kit (Bio-Rad, Hercules, USA). Real-time PCR was performed with iQ SYBR Green Supermix (Bio-Rad, Hercules, USA) and primers for IL-1β, IL-6 and TNF-α (Tsingke Biotechnology Co., Ltd.) and analyzed by the 2(-Delta Delta C(T)) method. β-actin served as the housekeeping gene. Real-time PCR was performed on an CFX 96 Real-time system (Bio-Rad, USA). The primer sequences are listed below: β-actin, CCCAAGGCCAACCGCGAGAAGAT and GTCCCGGCCAGCCAGGTCCAG; IL-1β, CACGATGCACCTGTACGATCA and GTTGCTCCATATCCTGTCCCT;

IL-6 TACCCCCAGGAGAAGATTCC and GCCATCTTTGGAAGGTTCAG; TNF-α, GGCTCCAGGCGGTGCTTGTTC and AGACGGCGATGCGGCTGATG.

Statistical analysis

Statistical differences of data were evaluated with two-tailed student's T-test by GraphPad Prism. The difference was considered to be significant when $P < 0.05$ (*), $P < 0.01$ (**) and $P < 0.001$ (***). Quantitative data were presented as mean ± standard deviation.

Results

Topical application of HCT ethanol extracts or its bioactive ingredient inhibits tumor growth

To prepare HCT ethanol extracts, we grounded the dry plant into powders, which were immersed in 95% ethanol to extract the soluble contents. The mixture was then centrifuged, filtered, lyophilized and weighted. The yield of ethanol extraction was 2.5% w/w. The product was then resuspended in DMSO to obtain a 41.67 mg/ml concentration, so that the final dose of 300 ml of drug applied onto each mouse (~25g) would be 500 mg/kg.

To examine HCT anti-cancer activity, we used two-stage model to induce SCC. Back skin of 6-Week-old female ICR mice were shaved and then topically applied with DMBA twice weekly for two weeks, followed by TPA twice weekly for six weeks, the time point when total tumor volume of most of mice reached ~100 mm^3. Mice with too small or large total tumor volume were excluded, and the left 14 mice with similar total tumor volume were selected and divided into HCT treatment and control groups. Thereafter, the mice were topically applied with 300 ml of HCT ethanol extracts or solvent DMSO as control daily for another three weeks. TPA application would be stopped during drug treatment.

During treatment, the mice of both groups remained in similar good physical condition. The mice body weight of the two groups occasionally fluctuated slightly during treatment, but the overall body weight of the mice remained unchanged (Fig. 1a, b). As revealed by tumor growth curves, HCT treatment significantly suppressed tumor growth (Fig. 1a, c). At the endpoint of treatment, the average total tumor volume of each mouse in HCT group reached 637 mm^3, which was much lower than that in control group with 1041 mm^3 ($P < 0.020$). In addition, tumor number of HCT group was lower than that of control group, indicating HCT also suppressed emergence of new tumors (Fig. 1d and 1f).

One of main bioactive ingredients of HCT is sodium houttuyfonate (SH). Due to the chemical instability of SH, its adduct analogue, sodium new houttuyfonate (SNH), has been synthesized to improve stability [27]. We then examined whether SNH had similar anti-cancer activity against SCC. As described above, mice with total tumor volume of ~100 mm^3 were divided into three groups and treated by 20 mg/kg SNH, 100mg/kg SNH and control solvent, respectively. As revealed by tumor growth curves, SNH treatment also efficiently suppressed tumor growth as well as number of new emerging tumors in a dose dependent manner (Fig. 1e and 1f). The overall body weight of the three groups of mice showed no difference (data

not shown). All of these data and observation demonstrate that topical application of the HCT extracts or its active ingredient efficiently suppresses SCC growth with low/no toxicity to the animals.

HCT treatment does not change known cancer promoting pathways

H&E staining showed similar architecture of tumor tissues from HCT and control groups (Fig. 2a). To investigate the molecular mechanism of how HCT inhibits SCC, we examined whether some known cancer promoting pathways were affected by HCT treatment. The protein b-Catenin is essential for skin cancer stem cells maintenance and SCC growth [28]. Western blot analysis showed that b-Catenin in HCT treatment group was statistically lower than that of control (Fig. 2b, c). However, there was huge variation between tumors even in the same group. Comprehensive genomic analysis of DMBA/TPA induced SCC have revealed that the vast majority of SCC possesses mutations in Hras, Kras or Rras2 [21]. Ras genes are often activated and play important roles during early stages of squamous cell carcinoma development [29, 30]. However, we didn't observe change of Ras downstream factor-ERK2 protein (Fig. 2b, c). The drug pump, ATP-binding cassette sub-family G member 2 (ABCG2), is well known as a specific marker of the "side population" (SP) of the cancer stem cells and is associated with drug resistance. ABCG2 could be controlled by several pathways, including the PI3K/Akt pathway [31]. ABCG2 protein expression varied between tumors, and there was no statistical difference between HCT group and control group (Fig. 2b, c). Since there was huge heterogeneity of protein expression between tumors, either in different mice or in different tumors from the same mice, it was difficult for us to obtain conclusive results. Therefore, we decided not to further pursue identifying signal pathways altered by HCT treatment.

Topical pretreatment of HCT ethanol extracts suppresses skin thickening induced by TPA

It has been reported that TPA alone could induce mouse ear skin oedema and this model has been used as a test for anti-inflammatory activity [32, 33]. Similar to ear skin, we found back skin swelling/thickening can be induced by TPA. To evaluate anti-inflammatory activity of HCT, mice back skin was pretreated daily with topical application of HCT for 10 days, followed by TPA (10 nmol/300 µL of DMSO) topical application daily for 3 days. The skin was then fixed by 4% *PFA, embedded in* paraffin, *sectioned and followed by* H&E staining. The skin thickness was defined by the distance from epidermis to the underlying fascia (Fig. 3a, 3b). The average skin thickness in HCT group reached 62.56 µm, which was significantly lower than that in control group with 84.68 µm (Fig. 3a, b, c). This result strongly indicates that HCT inhibits SCC through reducing skin inflammation during carcinogenesis.

HCT treatment reduces tumor infiltrating T cells

Since HCT is capable of reducing immune cells infiltrated into inflammatory tissues [25, 26], we then investigated whether HCT affects tumor microenvironments and examined tumor infiltrating T cells, which are recognized as the main effectors of antitumor immune responses [34]. Western blot analysis showed that the surface protein markers CD4 and CD8 of T cells were largely diminished in HCT treated tumors (Fig. 4a). Immunostaining analysis showed that there were abundant CD8^{+} cytotoxic T cells and

the CD4+ helper T cells infiltrated into cutaneous SCC tissues, especially in the stroma compartment (Fig. 4b and 4d). HCT treatment reduced both of these two types of T cells. The CD4+ helper T cells number was reduced much more than that of the CD8+ cytotoxic T cells after HCT treatment (Fig. 4b and 4c).

HCT treatment significantly increases the CD8+/Treg cells ratio

CD4+ T cells can be subdivided into regulatory T cells (Tregs) and traditional help T cells. Tregs, formerly known as suppressor T cells, suppress induction and proliferation of cytotoxic T cells, T helper cells and Antigen-Presenting Cells (APCs), therefore are detrimental to anti-tumor immune responses [35]. Tregs express the biomarker transcription factor Foxp3. Immunostaining results showed that most of CD4+ cells in tumors were Foxp3+ Tregs, and that CD4+, Foxp3+ Tregs number was significantly decreased after HCT treatment (Fig. 4d and 4e). In addition, CD8+/Treg cells ratio increased about 4 folds after HCT treatment (Fig. 4e).

HCT treatment on SCC cells reduces mRNA expression of inflammatory factors

To investigate the molecular mechanism of why skin inflammation as well as tumor infiltrating T cells were reduced after HCT treatment, we examined mRNA expression level of inflammatory factors in SCC cell line A431 treated by HCT in vitro. The real-time quantitative PCR analysis showed that the mRNA expression of IL-1β, IL-6 and TNF-α was only 11%, 8% and 19% of control group, respectively. These results indicate that HCT treatment might reduce the expression of inflammatory factors in skin cells, therefore reduce the recruitment of inflammatory cells, preventing skin tumorigenesis and suppressing SCC growth.

Discussion

In this work, we evaluated the anti-cancer activity of HCT and its bioactive ingredient in vivo using DMBA/TPA induced cutaneous SCC model. We have demonstrated that topical application of HCT reduces tumor infiltrating T lymphocytes, especially Tregs, increases CD8+/Treg cells ratio and efficiently suppresses tumor growth without obvious toxicity.

DMBA/TPA induced mice SCC is a unique in vivo cancer model, in which tumors on back skin can be directly visualized, quantitatively measured and traced individually over time. Since SCC has all of hallmarks of cancer development, including DNA mutation, genome instability, epigenetic changes, inflammation, oxidative stress and tumor microenvironment changes [16–19], our study not only demonstrates the anti-cancer activity of HCT on SCC in vivo, but more broadly, indicates HCT might have general anti-cancer activity on other cancer types in vivo.

Chemical induced SCC might develop through activating different cancer promoting pathways which are originated from different DNA mutations [21]. Therefore, it is no surprise that there is huge heterogeneity of protein expression levels between tumors, either from different mice or the same mouse. It is difficult to

come to a conclusion of which cancer promoting pathways are altered by HCT treatment, unless huge number of tumors are statistically analyzed.

HCT possesses anti-inflammatory activity [1, 2], and it is able to reduce inflammatory cell infiltration in different animal inflammation models [25, 26]. HCT treatment reverses oxaliplatin-induced neuropathic pain in rat by regulating Th17/Treg balance [36]. Consistent with previous reports, we found tumor infiltrating lymphocytes especially Tregs largely decreases, and $CD8^+$/Treg cells ratio increases after HCT treatment. Since Tregs dampers anti-cancer immune response through negatively regulating activation of effector T cells, significant increase of $CD8^+$/Treg cells ratio by HCT treatment can at least partially explain why HCT exhibits anti-cancer activity. In addition, change of infiltrating lymphocytes in tumors by HCT treatment indicates HCT might be able to change inflammatory cell infiltration during early stage of cancer development, therefore affects another process of cancer development. This was supported by the data that HCT pretreatment reduced the skin thickening/inflammation induced by TPA alone.

Since we topically applied the drug onto the tumor, it seems unlikely that HCT modulate the whole immune system and then affect the tumor infiltrating immune cells. Instead, our results support that HCT active components might penetrate into tumor tissue and directly impact on the cancer cells and immune cells around locally. Mechanistically, we have found that direct treatment on SCC cells in vitro by HCT could reduce the mRNA expression of IL-1β, IL-6 and TNF-α from SCC cells. This indicates that HCT might prevent skin tumorigenesis and suppress SCC growth through reducing the expression of inflammatory factors secreted from skin cells and therefore reducing the recruitment of inflammatory cells, including T lymphocytes.

HCT possesses activities against inflammation, oxidative stress and DNA mutations. All of these events are interconnected and play important roles in initiation and progression of cutaneous SCC. Although decrease of tumor infiltrating Tregs and increase of CD8+/Treg cells ratio can explain anti-cancer activity of HCT, we cannot exclude that other activities of HCT might also contribute to this anti-cancer effects. Nevertheless, our study provides another insight into molecular mechanism of HCT anti-cancer activity: it can re-balance the lymphocytes effector and suppressor infiltrated into tumor, therefore modulate the tumor immune microenvironment to counteract cancer cells.

In conclusion, our findings enhance understanding of molecular mechanism of HCT against tumorigenesis, and may lead to the development of new topical agents from HCT for the treatment of cutaneous SCC and other cancers.

Declarations

References

1. Kumar M, Prasad SK, Hemalatha S (2014) A current update on the phytopharmacological aspects of Houttuynia cordata Thunb. Pharmacogn Rev 8(15):22–35
2. Fu J, Dai L, Lin Z, Lu H (2013) Houttuynia cordata Thunb: A Review of Phytochemistry and Pharmacology and Quality Control. Chinese Medicine: 101-123
3. Tang YJ, Yang JS, Lin CF, Shyu WC, Tsuzuki M, Lu CC, Chen YF, Lai KC (2009) Houttuynia cordata Thunb extract induces apoptosis through mitochondrial-dependent pathway in HT-29 human colon adenocarcinoma cells. Oncol Rep 22(5):1051–1056
4. Liu J, Zhu X, Yang D, Li R, Jiang J (2020) Effect of Heat Treatment on the Anticancer Activity of Houttuynia cordata Thunb Aerial Stem Extract in Human Gastric Cancer SGC-7901 Cells. Nutr Cancer: 1-9
5. Yanarojana M, Nararatwanchai T, Thairat S, Tancharoen S (2017) Antiproliferative Activity and Induction of Apoptosis in Human Melanoma Cells by Houttuynia cordata Thunb Extract. Anticancer Res 37(12):6619–6628
6. Kim JM, Hwang IH, Jang IS, Kim M, Bang IS, Park SJ, Chung YJ, Joo JC, Lee MG (2017) Houttuynia cordata Thunb Promotes Activation of HIF-1A-FOXO3 and MEF2A Pathways to Induce Apoptosis in Human HepG2 Hepatocellular Carcinoma Cells. Integr Cancer Ther 16(3):360–372

7. Subhawa S, Chewonarin T, Banjerdpongchai R (2020) The Effects of Houttuynia cordata Thunb and Piper ribesioides Wall Extracts on Breast Carcinoma Cell Proliferation, Migration, Invasion and Apoptosis.Molecules25(5)

8. Lai KC, Chiu YJ, Tang YJ, Lin KL, Chiang JH, Jiang YL, Jen HF, Kuo YH, Agamaya S, Chung JG, Yang JS (2010) Houttuynia cordata Thunb extract inhibits cell growth and induces apoptosis in human primary colorectal cancer cells. Anticancer Res 30(9):3549–3556

9. Chen YF, Yang JS, Chang WS, Tsai SC, Peng SF, Zhou YR (2013) Houttuynia cordata Thunb extract modulates G0/G1 arrest and Fas/CD95-mediated death receptor apoptotic cell death in human lung cancer A549 cells. J Biomed Sci 20:18

10. Kwon KB, Kim EK, Shin BC, Seo EA, Yang JY, Ryu DG (2003) Herba houttuyniae extract induces apoptotic death of human promyelocytic leukemia cells via caspase activation accompanied by dissipation of mitochondrial membrane potential and cytochrome c release. Exp Mol Med 35(2):91–97

11. Lou Y, Guo Z, Zhu Y, Kong M, Zhang R, Lu L, Wu F, Liu Z, Wu J (2019) Houttuynia cordata Thunb. and its bioactive compound 2-undecanone significantly suppress benzo(a)pyrene-induced lung tumorigenesis by activating the Nrf2-HO-1/NQO-1 signaling pathway. J Exp Clin Cancer Res 38(1):242

12. Leiter U, Eigentler T, Garbe C (2014) Epidemiology of skin cancer. Adv Exp Med Biol 810:120–140

13. Gandhi SA, Kampp J (2015) Skin Cancer Epidemiology, Detection, and Management. Med Clin North Am 99(6):1323–1335

14. Apalla Z, Nashan D, Weller RB, Castellsague X (2017) Skin Cancer: Epidemiology, Disease Burden, Pathophysiology, Diagnosis, and Therapeutic Approaches. Dermatol Ther (Heidelb) 7(Suppl 1):5–19

15. Fahradyan A, Howell AC, Wolfswinkel EM, Tsuha M, Sheth P, Wong AK (2017) Updates on the Management of Non-Melanoma Skin Cancer (NMSC).Healthcare (Basel)5(4)

16. Voiculescu V, Calenic B, Ghita M, Lupu M, Caruntu A, Moraru L, Voiculescu S, Ion A, Greabu M, Ishkitiev N, Caruntu C (2016) From Normal Skin to Squamous Cell Carcinoma: A Quest for Novel Biomarkers. Dis Markers 2016: 4517492

17. Parekh V, Seykora JT (2017) Cutaneous Squamous Cell Carcinoma. Clin Lab Med 37(3):503–525

18. Nissinen L, Farshchian M, Riihila P, Kahari VM (2016) New perspectives on role of tumor microenvironment in progression of cutaneous squamous cell carcinoma. Cell Tissue Res 365(3):691–702

19. Marks F, Furstenberger G (1986) Experimental evidence that skin carcinogenesis is a multistep phenomenon. Br J Dermatol 115(Suppl 31):1–8

20. Abel EL, Angel JM, Kiguchi K, and J DiGiovanni (2009) Multi-stage chemical carcinogenesis in mouse skin: fundamentals and applications. Nat Protoc 4(9):1350–1362

21. Nassar D, Latil M, Boeckx B, Lambrechts D, Blanpain C (2015) Genomic landscape of carcinogen-induced and genetically induced mouse skin squamous cell carcinoma. Nat Med 21(8):946–954

22. Reagan-Shaw S, Nihal M, Ahmad N (2008) Dose translation from animal to human studies revisited. FASEB J 22(3):659–661

23. Balkwill FR, Capasso M, Hagemann T (2012) The tumor microenvironment at a glance. J Cell Sci 125(Pt 23):5591–5596

24. Kareva I (2019) Metabolism and Gut Microbiota in Cancer Immunoediting, CD8/Treg Ratios, Immune Cell Homeostasis, and Cancer (Immuno)Therapy: Concise Review. Stem Cells 37(10):1273–1280

25. Kim D, Park D, Kyung J, Yang YH, Choi EK, Lee YB, Kim HK, Hwang BY, Kim YB (2012) Anti-inflammatory effects of Houttuynia cordata supercritical extract in carrageenan-air pouch inflammation model. Lab Anim Res 28(2):137–140

26. Ling LJ, Lu Y, Zhang YY, Zhu HY, Tu P, Li H, Chen DF (2020) Flavonoids from Houttuynia cordata attenuate H1N1-induced acute lung injury in mice via inhibition of influenza virus and Toll-like receptor signalling. Phytomedicine 67:153150

27. Liu X, Zhong L, Xie J, Sui Y, Li G, Ma Z, Yang L (2021) Sodium houttuyfonate: A review of its antimicrobial, anti-inflammatory and cardiovascular protective effects. Eur J Pharmacol 902:174110

28. Malanchi I, Peinado H, Kassen D, Hussenet T, Metzger D, Chambon P, Huber M, Hohl D, Cano A, Birchmeier W, Huelsken J (2008) Cutaneous cancer stem cell maintenance is dependent on beta-catenin signalling. Nature 452(7187):650–653

29. Spencer JM, Kahn SM, Jiang W, DeLeo VA, Weinstein IB (1995) Activated ras genes occur in human actinic keratoses, premalignant precursors to squamous cell carcinomas. Arch Dermatol 131(7):796–800

30. Pierceall WE, Goldberg LH, Tainsky MA, Mukhopadhyay T, Ananthaswamy HN (1991) Ras gene mutation and amplification in human nonmelanoma skin cancers. Mol Carcinog 4(3):196–202

31. Westover D, Li F (2015) New trends for overcoming ABCG2/BCRP-mediated resistance to cancer therapies. J Exp Clin Cancer Res 34:159

32. Inoue H, Mori T, Shibata S, Koshihara Y (1989) Modulation by glycyrrhetinic acid derivatives of TPA-induced mouse ear oedema. Br J Pharmacol 96(1):204–210

33. Kang MR, Jo SA, Lee H, Yoon YD, Kwon JH, Yang JW, Choi BJ, Park KH, Lee MY, Lee CW, Lee KR, Kang JS (2020) Inhibition of Skin Inflammation by Scytonemin, an Ultraviolet Sunscreen Pigment.Mar Drugs18(6)

34. Yu P, Fu YX (2006) Tumor-infiltrating T lymphocytes: friends or foes? Lab Invest 86(3):231–245

35. Knutson KL, Disis ML (2005) Tumor antigen-specific T helper cells in cancer immunity and immunotherapy. Cancer Immunol Immunother 54(8):721–728

36. Wan CF, Zheng LL, Liu Y, Yu X (2016) Houttuynia cordata Thunb reverses oxaliplatin-induced neuropathic pain in rat by regulating Th17/Treg balance. Am J Transl Res 8(3):1609–1614
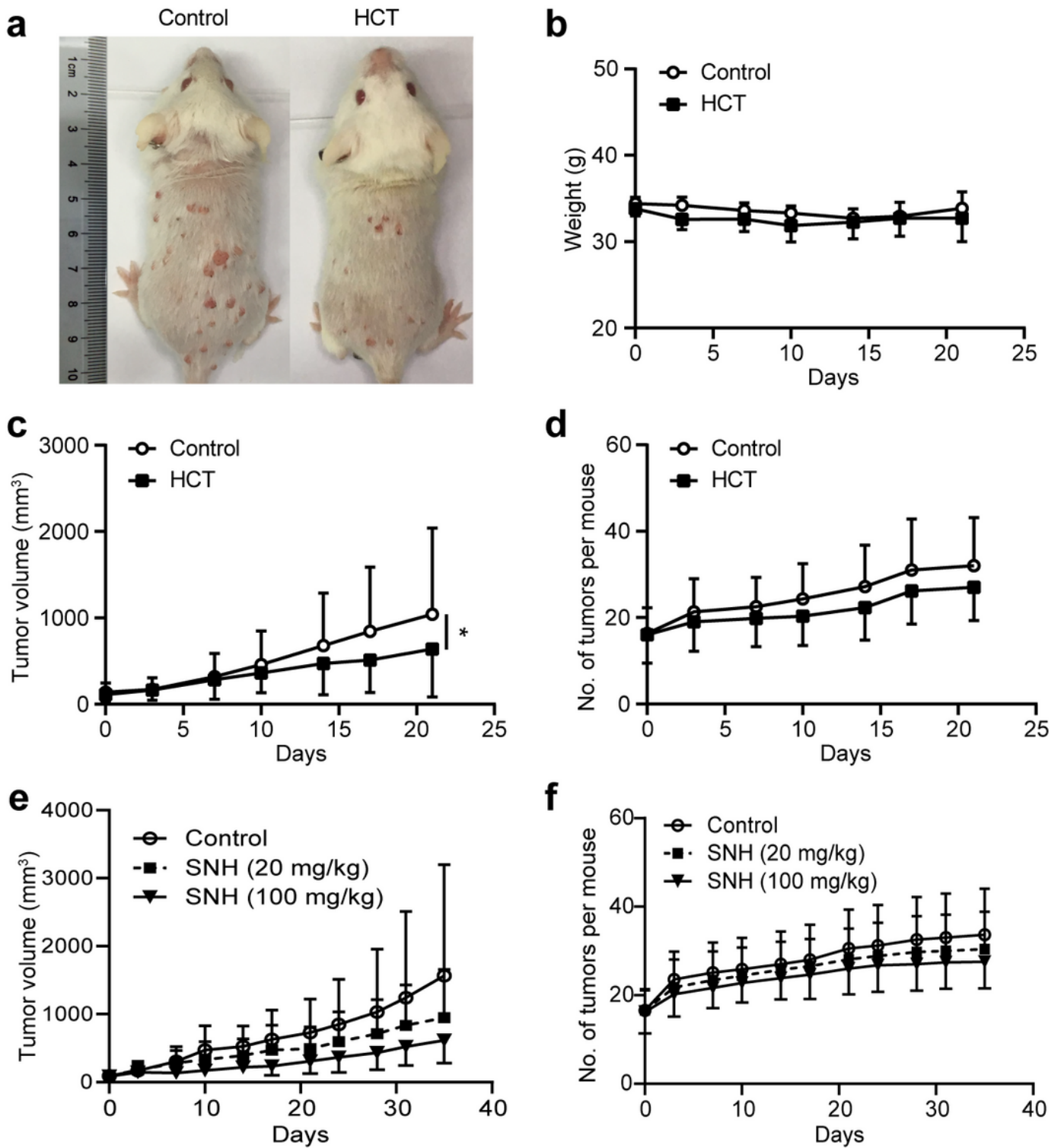
Figures

Figure 1

Houttuynia cordata Thunb ethanol extracts inhibits cutaneous SCC growth. Cutaneous SCC were induced by DMBA/TPA. When total tumor volume of most of mice reached ~100 mm^3, HCT or solvent DMSO were topically applied onto skin. Mice tumor volume and body weight were measured twice a week. **a** Representative images of back skin tumors in control and HCT groups. **b** The tumor growth curves of the HCT group and the control group. N = 7 mice. *P* = 0.020. **c** Tumor number of the HCT group and the

control group. **d** Body weight of HCT group and the control group over time. **e** The tumor growth curves of the SNH (20 mg/kg) group, SNH (100 mg/kg) group and control group. N = 9 mice. *P* = 0.209 (20 mg/kg SNH group and control group). *P* = 0.013 (100 mg/kg SNH group and control group). **f** Tumor number of the SNH (20 mg/kg) group, SNH (100 mg/kg) group and control group
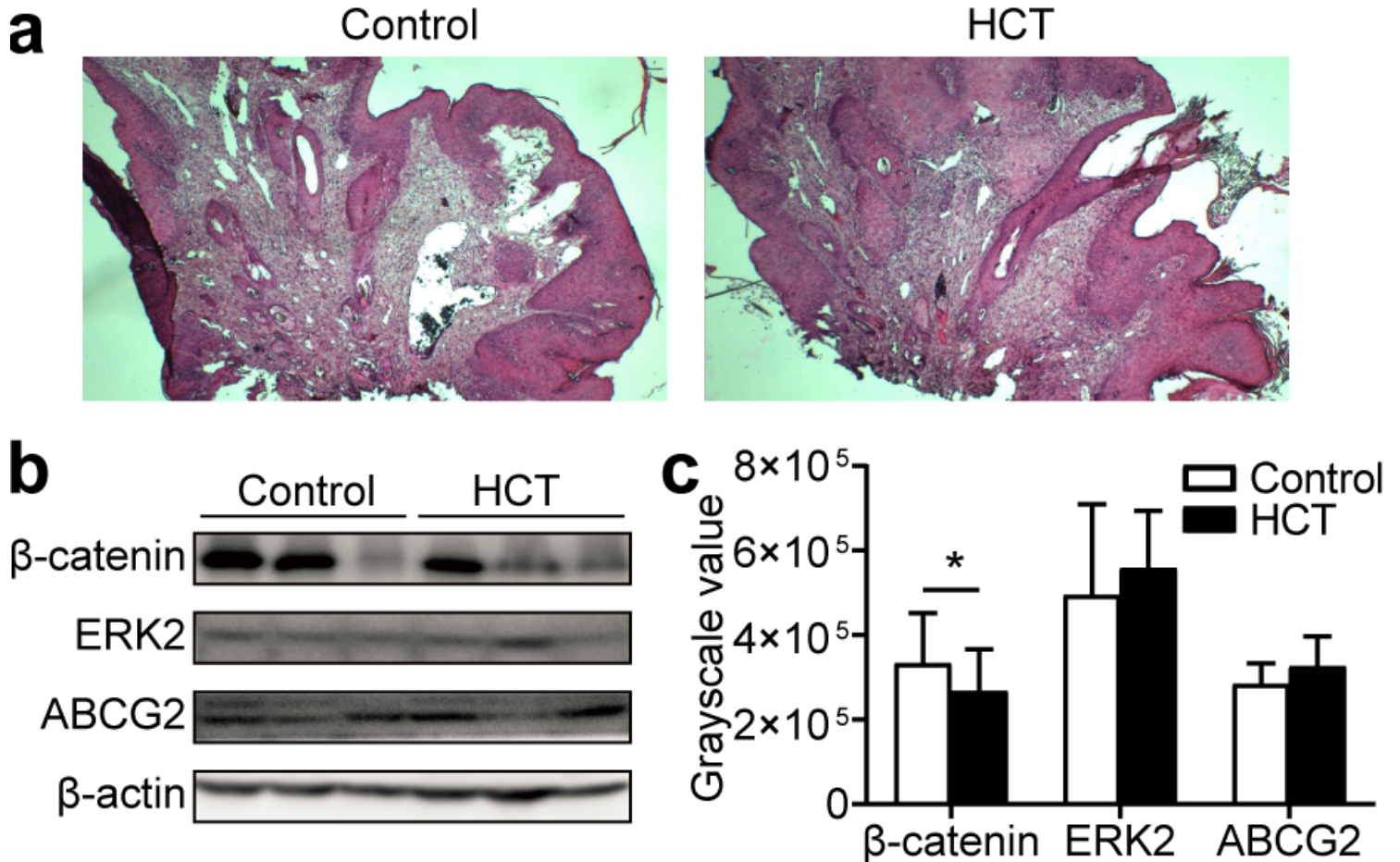

Figure 2

HCT treatment doesn't change known cancer promoting pathways. **a** H&E staining of tumor samples from HCT treatment or control group. **b** Proteins b-Catenin, ERK2, ABCG in tumors from HCT treatment or control group were analyzed by western blot. Actin was loaded as control. **c** Statistic quantification of western blot results. For b-Catenin, *P* = 0.020
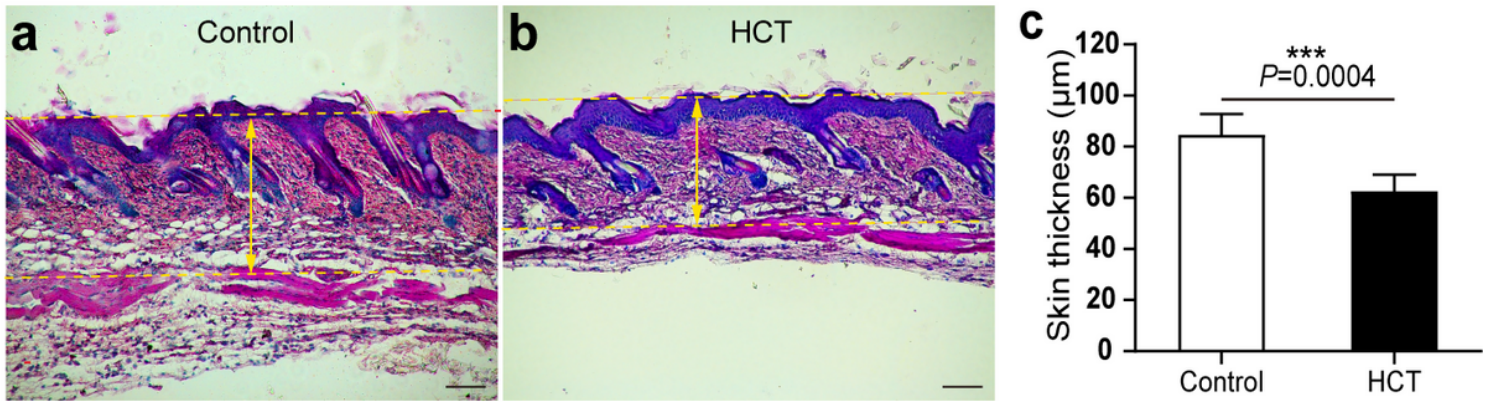
Figure 3

Pretreatment of HCT ethanol extracts suppresses skin thickening induced by TPA. Back skin of 6-Week-old female ICR mice were pretreated with topical application of HCT ethanol extracts for 10 days, followed by TPA topical application daily for 3 days. The skin was then fixed by 4% *PFA, embedded in* paraffin*, sectioned and followed by* H&E staining. **a, b** Representative H&E staining of back skin from control group and HCT group. The skin thickness was measured by the distance from epidermis to the underlying fascia (yellow arrows). Scale bar, 100 μm. **c** Statistic quantification of skin thickness. All fields in several sections of back skins from each mouse were counted. N = 6 mice. *P* = 0.0004
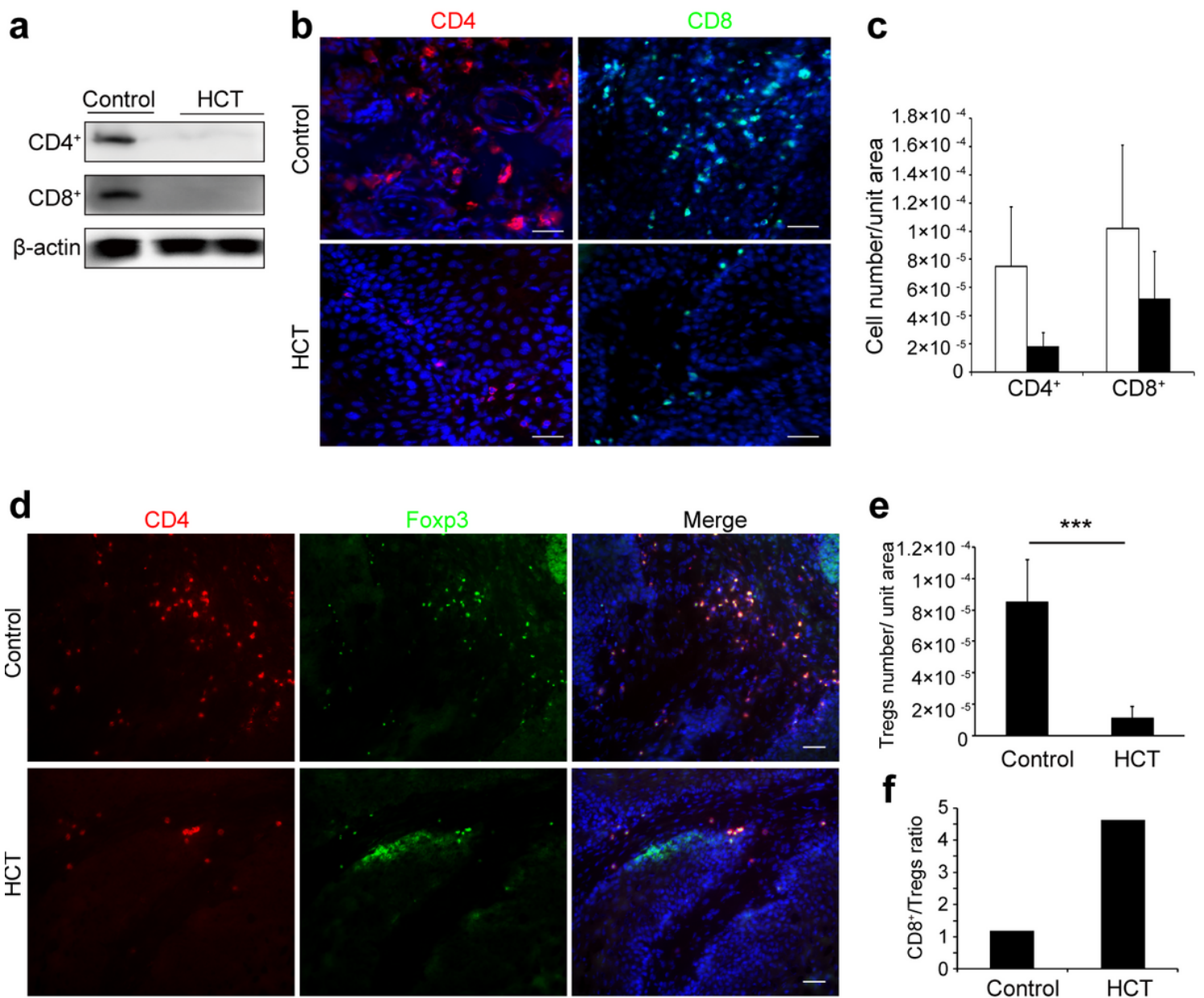
Figure 4

HCT treatment reduces tumor infiltrating T lymphocytes and increases the CD8^{+}/Treg cells ratio. **a** HCT treatment reduced the expression of CD4 and CD8 proteins in tumor samples, as analyzed by Western blot. **b** Representative immunofluorescence images of tumor infiltrating CD4^{+}and CD8^{+} cells from HCT treatment or control group. Tumors were frozen in OCT compound, sectioned and immunostained with Alexa Fluor 700 conjugated anti-CD4 antibody or Alexa Fluor 488 conjugated anti-CD8 antibody. **c** Statistic quantification of CD4^{+}and CD8^{+} cells number from HCT treatment or control group. All fields of CD4^{+} or CD8^{+} cells in several sections from each tumor were counted. N = 4 mice. For CD4^{+} cells, P = 0.058; For CD8^{+} cells, P = 0.210. Scale bar, 50 mm. **d** Representative immunofluorescence images of CD4^{+} and Foxp3^{+} cells in the tumors from the control and HCT groups. Tumor samples were frozen in OCT compound, sectioned and immunostained with Alexa Fluor 700 conjugated anti-CD4 antibody and

Alexa Fluor 488 conjugated anti-Foxp3 antibodies. Scale bar, 50 mm. **e** Statistic quantification of CD4$^+$, Foxp3$^+$ Tregs number from HCT treatment or control group. All fields of CD4$^+$, Foxp3$^+$ Tregs in several sections from each tumor were counted. N = 8 mice. *P* = 0.0002. **f** ratio of CD8$^+$ effector T cells number to CD4$^+$, Foxp3$^+$ Tregs number from HCT treatment and control groups
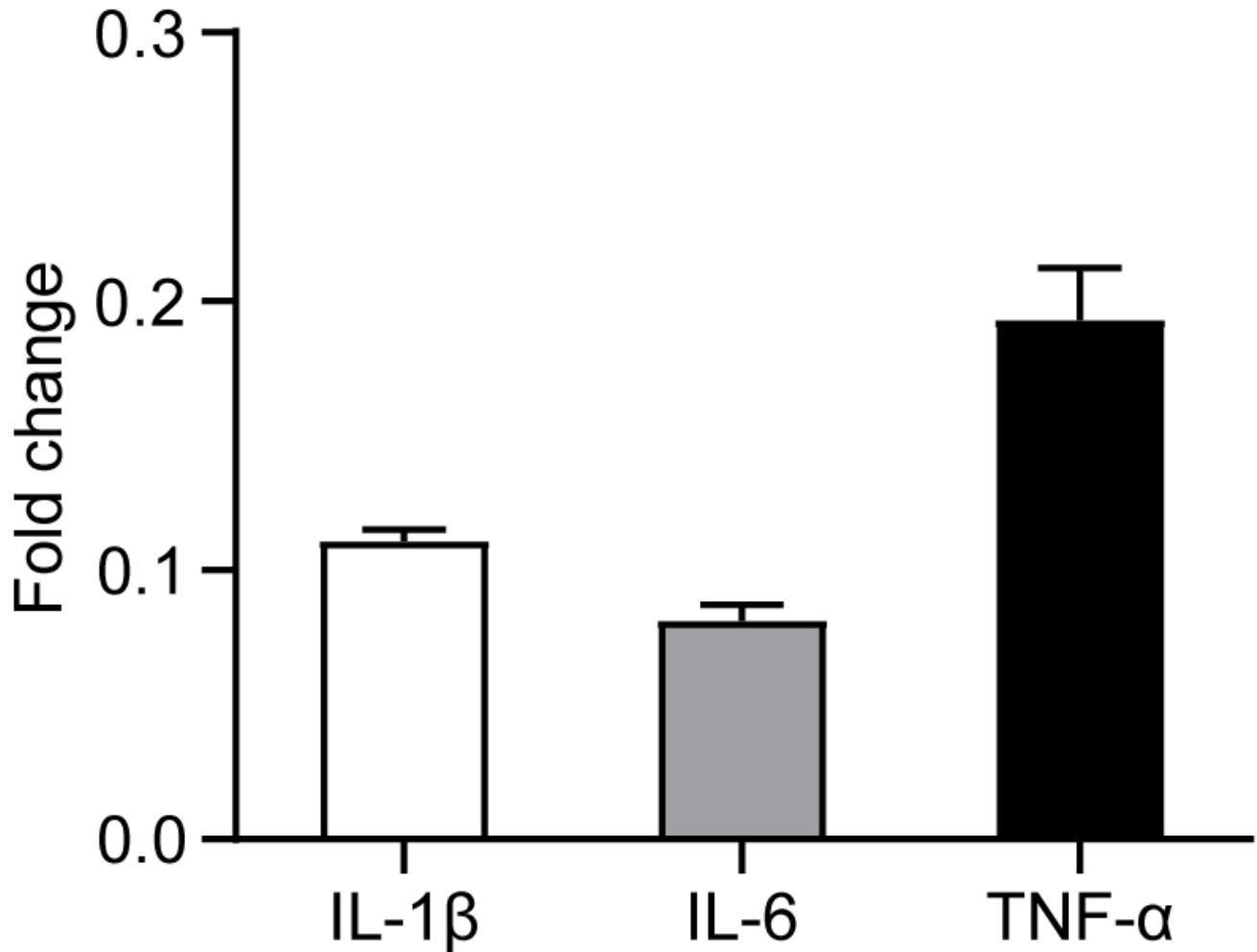

Figure 5

HCT treatment on SCC cells reduces mRNA expression of inflammatory factors. The mRNA expression of IL-1β, IL-6 and TNF-α in human A431 cells after HCT treatment were measured by real-time quantitative PCR. Each gene expression level from control group was normalized as 1. N = 3